ACS APPLIED MATERIALS & INTERFACES

Research Article

www.acsami.org

Different Organization of Type I Collagen Immobilized on Silanized and Nonsilanized Titanium Surfaces Affects Fibroblast Adhesion and Fibronectin Secretion

Nathalia Marín-Pareja,[†,§] Marco Cantini,[‡,§] Cristina González-García,[‡] Emiliano Salvagni,[†] Manuel Salmerón-Sánchez,[‡] and Maria-Pau Ginebra*[,†]

[†]Biomaterials, Biomechanics, and Tissue Engineering Group, Department of Materials Science and Metallurgy, Universitat Politècnica de Catalunya. BarcelonaTech (UPC), Av. Diagonal 647, 08028 Barcelona, Spain

[‡]Division of Biomedical Engineering, School of Engineering, University of Glasgow, Glasgow G12 8LT, U.K.

Supporting Information

ABSTRACT: Silanization has emerged in recent years as a way to obtain a stronger and more stable attachment of biomolecules to metallic substrates. However, its impact on protein conformation, a key aspect that influences cell response, has hardly been studied. In this work, we analyzed by atomic force microscopy (AFM) the distribution and conformation of type I collagen on plasma-treated surfaces before and after silanization. Subsequently, we investigated the effect of the different collagen conformations on fibroblasts adhesion and fibronectin secretion by immunofluorescence analyses. Two different organosilanes were used on plasma-treated titanium surfaces, either 3-chloropropyl-triethoxy-silane (CPTES) or 3-glycidyloxypropyl-triethoxy-silane (GPTES). The properties and amount of the adsorbed collagen were assessed by contact angle, X-ray photoelectron spectroscopy, optical waveguide lightmode spectroscopy, and AFM. AFM studies revealed different conformations of type I collagen depending on the silane employed. Collagen was organized in fibrillar networks over very hydrophilic (plasma treated titanium) or hydrophobic (silanized with CPTES) surfaces, the latter forming little globules with a beads-on-a-string appearance, whereas over surfaces presenting an intermediate hydrophobic character (silanized with GPTES), collagen was organized into clusters with a size increasing at higher protein concentration in solution. Cell response was strongly affected by collagen conformation, especially at low collagen density. The samples exhibiting collagen organized in globular clusters (GPTES-functionalized samples) favored a faster and better fibroblast adhesion as well as better cell spreading, focal adhesions formation, and more pronounced fibronectin fibrillogenesis. In contrast, when a certain protein concentration was reached at the material surface, the effect of collagen conformation was masked, and similar fibroblast response was observed in all samples.

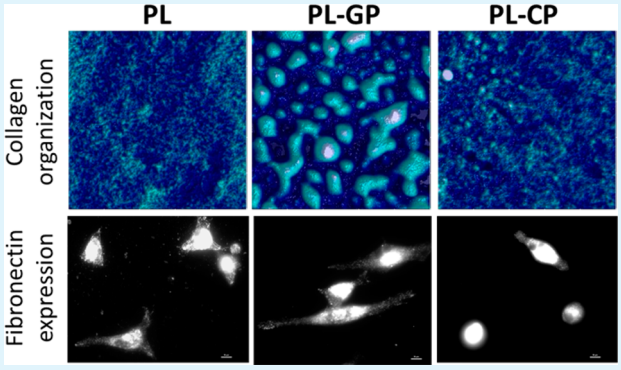

KEYWORDS: *collagen conformation, atomic force microscopy, silanization, fibronectin, fibroblast, adhesion, titanium, dental implant*

1. INTRODUCTION

An appropriate cellular response to implant surfaces is essential for a good *in vivo* performance. Dental implants interact both with bone and gingival tissues. Although bone integration is essential to ensure a good mechanical fixation of the implant, the good integration with the mucosal tissue of the gingiva is critical to guarantee a good biological sealing, which avoids bacteria colonization of the dental implant.[1−3] Surface functionalization with extracellular matrix (ECM) proteins has proven to be a good strategy to provide cellular attachment sites.[4−6] Recently, the immobilization of type I collagen, the main constituent of the gingival tissue, on implant surfaces has been described as a route to improve fibroblast response and to accelerate the healing processes of the gingival mucosal tissue.[7−9]

The chemistry of the underlying substrate (particularly as it affects wettability and surface charge) has a significant effect on the structural features of the adsorbed protein layer.[10−12] Interfacial electrostatic and hydrophobic interactions can be large enough to significantly alter the density, conformation, orientation, and mobility of the proteins that make up the adsorbed layer.[13,14] Several studies have shown the effect of surface chemistry on the adsorption of ECM proteins, such as fibronectin,[15,16] fibrinogen,[17] and laminin,[18] and how alterations in protein adsorption can influence fibroblast response.[19,20] At the same time, surface-induced alterations in protein structure can greatly influence the nature of the ligands

Received: June 18, 2015
Accepted: August 31, 2015
Published: August 31, 2015

DOI: 10.1021/acsami.5b05420
ACS Appl. Mater. Interfaces 2015, 7, 20667−20677

and other ECM signals presented to the cells.[21] Several studies using alkanethiol self-assembled monolayers with different functional groups (CH_3, OH, COOH, and NH_2) have been performed to determine the effects of surface properties on cell response.[11,19,22,23] Most of these studies examine the effect of surface chemistry on wettability and subsequent effects on protein adsorption and cell adhesion by the number of adherent cells, morphology, and immunofluorescent staining after several hours of incubation.

More specifically, the effect of substrate surface chemistry on the adsorption of collagen from solution has been addressed in other studies, concluding that the amount of adsorbed collagen and its structure are particularly influenced by the wettability of the surface.[10−12,24−27] Besides physisorption, covalent binding of proteins through the use of silanes has emerged in recent years as an attractive way to functionalize metallic substrates.[28,29] In this strategy, a pretreatment of the surface is performed to facilitate the formation of covalent bonds between the protein and the substrate. Organosilanes exhibit a "tail" capable of binding the hydroxyl groups present on the metal surface and, in the other end, a "head" functional group for binding the desired molecules. The advantage of this approach, compared to physisorption, is that it may offer a stronger and more stable attachment of biomolecules.[7,8,29−33] Previous studies have demonstrated through several analytical techniques (X-ray photoelectron spectroscopy (XPS), fluorescence labeling) that collagen immobilized on silanized titanium surfaces exhibited a significantly higher stability than physisorbed collagen, suggesting that covalent binding was occurring at the metal surface.[29] In addition to producing more stable bonds and affecting the amount of immobilized protein, the novel surface chemistry is expected to affect the conformation of the protein.

Even if some efforts have been devoted to study the effect of some surface properties on the morphology of adsorbed collagen (type I and IV) and cell response,[11,27,34−36] the influence of silanized titanium surfaces on type I collagen conformation and their subsequent effect on fibroblast behavior have not been addressed yet. In this study, we focus specifically on how silanization, which is aimed at obtaining a stronger bonding between collagen and the surface, influences the distribution and conformation of type I collagen and in turn affects fibroblasts adhesion and fibronectin secretion. We used several methods to prepare substrates with systematic variations in surface chemistry and examined the properties and amount of the adsorbed collagen with contact angle, XPS, optical waveguide lightmode spectroscopy (OWLS), and atomic force microscopy (AFM). Fibroblast adhesion and fibronectin fibrillogenesis were also evaluated through immunofluorescence analyses.

2. MATERIALS AND METHODS

2.1. Titanium Preparation. The samples used in this study were commercially pure grade 2 titanium (Ti) discs with 9 mm diameter and 2−3 mm thickness (Zapp AG, Ratingen-Germany). The surface was finished and polished with 1200 and 4000 grit silicon carbide paper and subsequently with colloidal silica (0.06 μm). Then, the discs were immersed in a sodium hydroxide−acetone solution (Sigma−Aldrich, Madrid-Spain) and washed in an ultrasonic bath for 5 min, followed by further cleaning by ultrasonication in cyclohexane, isopropanol, ethanol, deionized water (Mili-Q Plus), and acetone (Sigma−Aldrich, Madrid, Spain) to remove organic and inorganic impurities. After the samples were dried with N_2 gas, the polished surfaces were activated in an O_2 plasma cleaner (PDC-002, Harrick Scientific Corporation, USA) for 5 min (PL). This treatment effectively removes contaminants and forms reactive hydroxyl groups on the surface, beneficial for further chemical modification.

2.2. Silanization. The clean plasma-pretreated Ti surfaces were silanized using two different oragnosilanes, either 3-chloropropyl-triethoxy-silane (CPTES) or 3-glycidyloxypropyl-triethoxy-silane (GPTES). The samples were divided in two groups and immersed for 1 h at room temperature (RT) in a pentane solution containing either (i) 0.05 M N−N diisopropyl-ethyl-amine (DIEA) and 0.5 M CPTES, which has a chlorine (-Cl) as a functional group, or (ii) 0.5 M GPTES, which has an epoxy group ($-CHCH_2O$) as a functional group. All chemicals were purchased from Sigma-Aldrich, Madrid, Spain. Afterward, the silanized samples were ultrasonicated successively in isopropanol, ethanol, deionized water (Mili-Q Plus), and acetone to remove noncovalent surface bound adsorbed molecules and were dried with N_2 gas.

2.3. Collagen Immobilization. Type I collagen was immobilized on the plasma-pretreated samples and on the samples silanized either with CPTES or GPTES. Type I collagen, obtained from bovine pericardium as described elsewhere,[37] was dissolved in acetic acid 0.05 M, and the pH was adjusted to ∼6 with sodium hydroxide 0.01 M. Solutions with different concentrations of collagen (between 2.5 and 150 μg/mL) and same pH ≈ 6 were prepared to evaluate the evolution of collagen immobilization as a function of collagen concentration. The samples were immersed into these solutions, during different adsorption times, to evaluate the effect of these conditions onto collagen morphology over the surface. After the samples were removed from the solution, they were rinsed twice with a 0.05 M acetic acid solution to remove excess of adsorbed collagen and were dried under N_2 flow. The nomenclature used throughout the article to identify the different surfaces studied is summarized in Table 1.

Table 1. Nomenclature for Modified Ti Surfaces

groups	sample description
Ti	commercially pure Ti, untreated (just polished)
Activated	
PL	polished Ti treated with oxygen plasma cleaner
Silanized	
PL-CP	PL followed by silanization with CPTES
PL-GP	PL followed by silanization with GPTES
Collagen-Coated	
PL-col	PL with collagen (physisorption)
PL-CP-col	PL-CP with collagen (covalent immobilization)
PL-GP-col	PL-GP with collagen (covalent immobilization)

2.4. Surface Characterization. *2.4.1. Contact Angle.* To determine the wettability of the different substrates, static contact angle measurements were performed using the sessile drop method[38] in a contact angle video based system OCA15plus Video-Based Contact Angle System (Dataphysics, Germany) and analyzed with the SCA20 software (Dataphysics Instruments GMBH, Germany). The liquid used for contact angle measurements was Milli-Q water (Milli-Q, Millipore, Germany) at RT. Samples were introduced in a water vapor saturated chamber, and 3 μL drops were deposited at random over the substrate surface. Contact angles were measured immediately after drop deposition. Three readings were taken on each test specimen, and the experiment was performed in triplicate for each condition.

2.4.2. Surface Analysis by XPS. The samples were analyzed by XPS after plasma treatment and subsequent silanization with CPTES or GPTES. XPS was performed with a SPECS system equipped with an Al anode XR50 source operating at 150 W and a Phoibos 150 MCD-9 detector XP. Samples were directly fixed onto the sample holder with double-sided carbon tape. Spectra were recorded with pass energy of 25 at 0.1 eV steps at a pressure below 6×10^{-9} mbar, and binding energies were referred to the C 1s signal. The binding energies were corrected by referencing the adventitious C 1s peak maximum at 284.8

DOI: 10.1021/acsami.5b05420
ACS Appl. Mater. Interfaces 2015, 7, 20667−20677

Table 2. XPS Characterization. Atomic Percentages of the Untreated (Ti), Plasma-Treated (PL), and Silanized Samples (PL-CP and PL-GP). Numbers in Brackets Indicate Standard Deviation

	element (atomic %)						
sample	C 1s	N 1s	O 1s	Si 2p	Cl 2p	Ti 2p	Na 1s
Ti	33.2 (3.3)	0.1 (0.1)	27.8 (1.6)	0.2 (0.2)	0.0	3.5 (0.3)	35.1 (1.3)
PL	10.0 (3.7)	1.6 (0.4)	48.0 (2.3)	2.1 (1.0)	0.2 (0.1)	16.9 (0.7)	21.5 (3.6)
PL-CP	21.6 (2.0)	0.6 (0.4)	49.5 (0.6)	4.8 (0.3)	2.3 (0.1)	11.4 (1.3)	9.5 (0.6)
PL-GP	15.6 (2.8)	0.8 (0.4)	53.9 (0.8)	3.4 (0.6)	0.4 (0.0)	13.4 (1.3)	12.4 (2.8)

eV for all the specimens used in this study. Measured intensities (peak areas) were converted to normalized intensities by atomic sensitivity factors from which atomic compositions of surfaces were calculated. The average values obtained from three substrate replicates are reported.

2.4.3. OWLS. To measure the amount of adhered collagen on each of the modified titanium surfaces, the adsorption process at the solid/liquid interface was assessed using an OWLS instrument (OWLS2400 MicroVacuum, Budapest- Hungary). This technique detects changes in the effective refractive index occurring within a sensor, and these changes are converted into adsorbed mass using the de Feijter's formula.[39] The optical grating coupler sensor chip consisted of SiO_2 as base substrate, coated with TiO_2. Prior to measurements, the TiO_2-coated sensor waveguides were subjected to oxygen plasma and silanized as described earlier. To obtain a stable baseline, the clean sensor was incubated at RT in a 10 mM *N*-(2-hydroxyethyl)-piperazine-*N*′-ethanesulfonic acid (HEPES) buffer solution supplemented with 150 mM NaCl until the signal was stabilized. Temperature was equilibrated at 37 °C until the signal was stabilized. Afterward, the collagen solution was injected and left in contact with the waveguide for 10 min and overnight to monitor collagen adsorption at different time points and collagen concentrations. Subsequently, the waveguide was rinsed with acetic acid to remove unbound collagen, after which HEPES buffer solution was injected until signal stabilization. The uncoupling angles, RTM and RTE, were recorded and converted to refractive indices (NTM, NTE) by the manufacturer supplied software. The experiment was performed in triplicate for each condition.

2.4.4. AFM. The NanoScope III AFM from Digital Instruments (Santa Barbara, CA, USA) was used in the tapping mode in air to follow the collagen adsorption profile and the morphology of the adsorbed protein layer. Si cantilevers from Veeco (Manchester, UK) were used, with a force constant of 2.8 N/m and a resonance frequency of 75 kHz. The phase signal was set to zero at the resonance frequency of the tip. The tapping frequency was 5−10% lower than the resonance frequency. Drive amplitude was 200 mV, and the amplitude set-point was 1.4 V. The ratio between the amplitude set-point and the free amplitude was kept equal to 0.7. Several AFM images were analyzed using the NanoScope software (version 1.4 of 2011) to observe the topography of uncoated titanium surfaces as well as that of collagen-coated samples.

AFM was used to evaluate how the different treatments performed on the titanium surfaces affect the morphology of adsorbed collagen. Each treatment can influence both the dynamics of adsorption and the distribution of collagen upon adsorption. Therefore, several protein concentrations (between 2.5 and 150 μg/mL) were evaluated, setting the immersion time at 10 min. With these studies, we wanted to determine the minimal collagen concentration necessary in each case to observe the collagen distribution and conformation and to follow the dynamics of protein adsorption on the surfaces. Particle analysis was performed using the NanoScope software (version 1.4 of 2011) to identify the presence, size, and distance of clusters on the collagen-coated surface.

2.5. Cell Adhesion Studies. *2.5.1. Cell Culture.* Prior to culture, all samples were immersed in a 1% bovine serum albumin solution (BSA, Sigma-Aldrich) in phosphate buffered saline (PBS, Invitrogen) for 30 min to avoid unspecific protein binding. Human dermal fibroblasts (HDFs) were incubated on the samples at a concentration of 5000 cells/sample with serum-free medium (Dulbecco's modified Eagle's medium, DMEM) supplemented with 1% L-glutamine and 1% penicillin/streptomycin at 37 °C with 5% CO_2 for 4 h. Four to six passage cells were used in all experiments. All the experiments were performed twice, with three samples per group. Cell adhesion and spreading on the different Ti surfaces were evaluated by immunostaining, as detailed in the following sections. Additionally, cell proliferation was assessed in the samples that had been previously immersed in 150 μg/mL collagen solution. HDF cells were seeded on the tested surfaces at a density of 32×10^3 cells/cm^2 and incubated for 4 h in serum-free medium. Then, the medium was replaced with serum-containing one (10% fetal bovine serum, FBS), and the cells were cultured for 1, 3, and 7 days. Untreated titanium discs were used as a control. Cell number was evaluated by lactate dehydrogenase assay as detailed elsewhere.[29]

2.5.2. Immunofluorescence. After 4 h of culture, the culture medium was removed, and unattached cells were washed away from the surface with PBS. Cells were fixed with 3% paraformaldehyde in PBS for 30 min at 4 °C and washed three times with PBS. After being permeabilized with 0.1% Triton-X in PBS for 5 min at RT and blocked with DPBS/BSA 1% at RT for 30 min, samples were incubated with a primary antibody for 1 h at RT; the antibody used to analyze vinculin expression was antivinculin (mouse) (hVIN-1, Sigma-Aldrich) 1:400 in DPBS/BSA 1% and to analyze fibronectin expression was antifibronectin (rabbit) (polyclonal, Sigma-Aldrich) 1:400 in DPBS/BSA 1%. Samples were washed twice with DPBS/Tween 20. A combination of secondary antibody (Cy3-conjugated goat antimouse or antirabbit, respectively, Jackson ImmunoResearch) and phalloidin (1:100) (BODIPY FL, Life Technology) was added and incubated by 1 h at RT. Finally, after the samples were washed with DPBS/Tween 20 three times, a mounting with Vectashield solution containing 4',6-diamidino-2-phenylindole (DAPI) (Vector Laboratories) was performed.

2.5.3. Analysis of Cell Images. Cells were visualized and photographed using a fluorescence microscope (NIKON, Japan) and analyzed using the ImageJ software. To determine cell density, four images at low magnification (4×) were acquired per sample, which covered the entire area of the sample. Morphological parameters were assessed at higher magnification (20×, 40×, and 60×). A minimum of three representative images were acquired per sample, this giving a minimum of nine images per experimental condition. Cell area and circularity were measured on a minimum of five cells per image. The length and number of early fibronectin fibrils were analyzed by adapting a published procedure for the analyses of focal adhesion number, size, and length.[40,41] Images of fibronectin expression were analyzed, and only features with an eccentricity higher than 0.95 were considered and identified as fibrillar-like structures.

2.6. Statistical Analysis. The experiments for the physical and chemical characterization of the samples were performed in triplicate. Cell culture experiments were performed twice, with three replicates per group. Results are displayed as mean ± SD. Analysis of variance (ANOVA)-tables with multiple comparison Fisher's test were used to determine statistically significant (p-value <0.05) differences between the means of the different groups.

3. RESULTS AND DISCUSSION

3.1. XPS. XPS analyses of the different titanium surfaces are summarized in Table 2. The samples were analyzed after each reaction step, and untreated pure titanium (Ti) was included as

DOI: 10.1021/acsami.5b05420
ACS Appl. Mater. Interfaces 2015, 7, 20667−20677

a control. A strong decrease in the carbon content was observed after plasma treatment (PL) compared to the untreated titanium (Ti), ascribed to the removal of organic contaminants from the atmosphere.[38] The amount of oxygen increased, consistent with surface cleaning and oxidation. The presence of Na was attributed to contamination caused by the use of NaOH as a cleaning agent, and it decreased after activation and silanization. The presence of small amounts of Si in the Ti and PL samples was due to contamination from the polishing with silicon carbide, whereas the significant increase of Si in the silanized samples (PL-CP, PL-GP), and Cl in the PL-CP, together with a decrease in the levels of Ti is indicative of the formation of a silane layer and a good coverage of the metal surface. As expected, C content increased also in the silanized samples due to the presence of the alkyl chain of the organosilanes, whereas Ti levels decreased in comparison to plasma-treated samples.

The deconvolution of the high-resolution XPS curve of O 1s (Figure 1 and Table 3) shows the evolution of this peak before

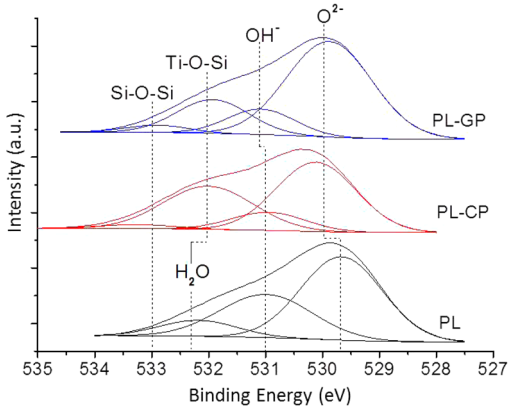

Figure 1. High-resolution spectra of the O 1s peak obtained for the plasma-treated and silanized samples.

and after silanization. At least four contributions to this peak were identified. O^{2-} at a binding energy (BE) of 529.9 (peak 1), OH at a BE of 531.0 (peak 2), the combination of H_2O/Ti−O−Si at a BE of 532.2 (peak 3). Moreover, another contribution at around 533 eV was attributed to Si−O−Si (peak 4) bonds.[42,43] PL-CP and PL-GP samples showed an increase in the peak 3 at a binding energy of 532.2 eV, assigned to the Ti−O−Si bonds, thus proving covalent bonding between the organosilane and the metal surface.[29,43,44] The percentages corresponding to hydroxyl groups (peak 2, ~531 eV) decreased significantly after silanization. To compare relative surface coverage among samples, the ratios between peaks 3 and 4 over peaks 1 and 2 ($ratio_{(3+4)/(1+2)}$) were evaluated. The atomic percentages of peaks 3 and 4 species in the PL-CP sample, as well as the $ratio_{(3+4)/(1+2)}$, were higher than in the PL-GP sample, thus suggesting a higher silanization coverage for PL-CP surfaces (Table 3).

3.2. Contact Angle. The water contact angle was measured to assess the influence of wettability on the morphology that collagen adopts on the different Ti surfaces. Untreated Ti samples had a contact angle close to 50°, which was strongly reduced after PL treatment, the surface becoming highly hydrophilic (Figure 2). The increase in the hydrophilicity of the

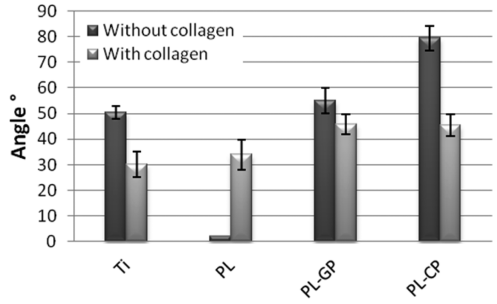

Figure 2. Contact angle of the different modified titanium surfaces before and after collagen immobilization.

PL samples can be attributed to the hydroxyl groups introduced on the Ti surfaces and to the removal of the adsorbed contaminants such as hydrocarbons, which tend to increase the hydrophobicity of the surface.[45] After the silanization processes, the surfaces became more hydrophobic due to the presence of alkyl chains with hydrophobic properties in the organosilanes. This effect was more pronounced for PL-CP than for PL-GP. The hydrophobic character of silane depends on different factors such as the organofunctional group of each silane and the conditions used for their deposition, which may result in a monolayer or a polymerized layer deposition.[46] In the case of organofunctional group, the chlorine (Cl) present in CPTES has a hydrophobic character, whereas the epoxy group present in GPTES is more hydrophilic due to the presence of an oxygen that can establish hydrogen bonds with water at the surface. Moreover, silanized GPTES surfaces resulted in a lower amount of silane molecules than silanized CPTES surfaces as shown by XPS measurements (Tables 2 and 3). This can partially leave free OH^- groups to interact with water leading to lower contact angles. After collagen immobilization, all surfaces presented intermediate contact angle values, which are slightly higher for the collagen silanized samples. This finding is consistent with the presence of hydrocarbon chains and hydrophilic functional groups in the collagen molecules,[47]

Table 3. Atomic Percentage of Species Present in the O 1s Peak of the Samples Treated with Plasma and Silanized

O 1s peak deconvolution			PL	PL-CP	PL-GP
			O 1s general percentage		
			48	49.5	53.9
peak	bond	BE (eV)	sub peaks percentage		
1	O^{2-}	529.9 ± 0.2	25.2	24.8	34.5
2	OH^-	531.0 ± 0.1	17.9	5.0	7.2
3	H_2O/Ti−O−Si	532.2 ± 0.2	4.9	17.4	10.3
4	Si−O−Si	533.2 ± 0.1	0	2.3	1.9
(3 + 4)/(1 + 2)				0.7	0.3

DOI: 10.1021/acsami.5b05420
ACS Appl. Mater. Interfaces 2015, 7, 20667−20677

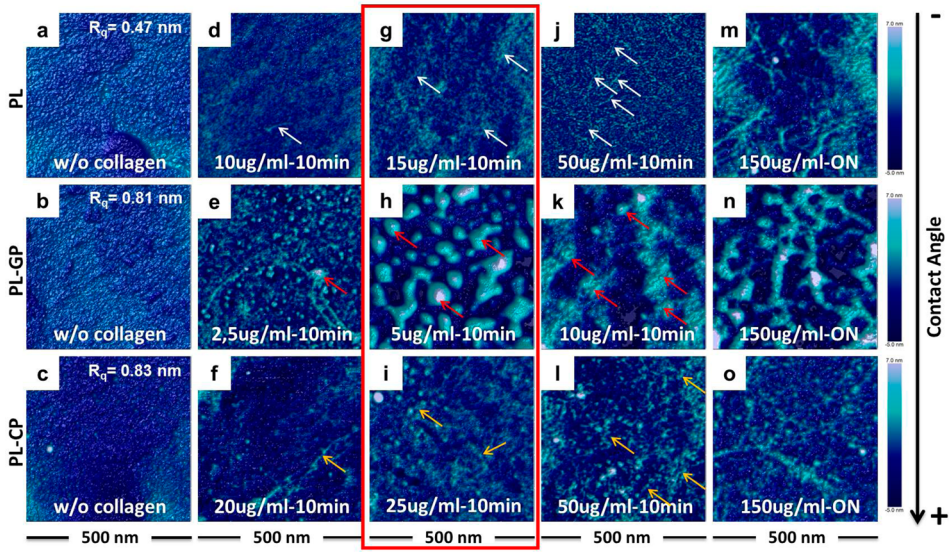

Figure 3. Evolution of the morphology of collagen adsorbed on chemically modified titanium surfaces, PL (upper row), PL-GP (second row), and PL-CP (bottom row), after 10 min of immersion in collagen solutions with increasing concentrations, as observed by height signal in tapping mode AFM. The red box indicates the minimal collagen concentrations where collagen was clearly visible on Ti surfaces, corresponding to 15 μg/mL for PL (g), 5 μg/mL for PL-GP (h), and 25 μg/mL for PL-CP (i). All images have the same lateral size (500 nm) and the same height range (max, 7 nm; min, −5 nm). Distinct morphologies are observed on the different surfaces: smooth collagen fibers on PL (white arrows), rougher fibers showing a beads-on-a-string morphology on PL-CP surfaces (yellow arrows), and globular clusters on PL-GP surfaces (red arrows).

and with the fact that underlying silanes can be partially exposed on the surface.

3.3. AFM. AFM analysis showed representative images of the evolution of collagen morphology on the different surfaces (Figure 3). All images of collagen-coated samples were compared to the noncoated samples (Figure 3a–c). The dynamics of collagen adsorption were different on each surface, as revealed by the minimum concentration needed to clearly detect collagen on the surface after 10 min of adsorption. On PL-GP surfaces, collagen was adsorbed from solutions of lower concentrations, indicating faster dynamics of protein adsorption. At 5 μg/mL, the presence of collagen on the surface is already clear. On the other hand, the minimum concentration at which collagen was visible on the surface was 15 μg/mL for PL and 25 μg/mL for PL-CP. Moreover, adsorbed collagen adopted different morphologies on the surfaces: on PL and PL-CP samples, collagen formed fibrillar nanonetworks, whereas on PL-GP samples, interconnected globular clusters were observed. In the case of PL-CP samples, these fibers have a beads-on-a-string morphology. Analyses of particle size and distribution for PL-GP surfaces at this minimum concentration revealed an average spacing between clusters of 75.99 ± 0.43 nm; on the other hand, no regular structures could be identified on PL-CP and PL samples.

At low concentrations, collagen molecules were difficult to visualize (Figure 3d–f). As concentration increased, the increase of adhered collagen gradually led to coverage of the entire surfaces (Figure 3j–l). On PL (Figure 3d,g,j, white arrows) and PL-CP samples (Figure 3f,i,l, yellow arrows), the thickness of fibers increased with the increase of concentration, and on PL-GP samples, the globular clusters enlarged and tended to connect to each other (Figure 3e,h,k, red arrows). Increasing of concentration to 150 μg/mL and the immersion time to 16 h (ON: overnight) led to an increase in the length and thickness of the fibers on treated plasma and silanized CPTES samples (Figure 3m,o), whereas on silanized GPTES samples, the globular aggregates became lengthened and connected (Figure 3n). Multiple layers of protein are likely to be formed.

Some parameters that have been shown to influence the morphology of immobilized biomolecules are surface chemistry and wettability.[10−12,24−26] In our case, both highly hydrophilic PL samples and highly hydrophobic PL-CP samples induced the formation of a network of collagen nanofibers. In the case of hydrophilic PL surfaces, collagen formed smoother fibers, whereas on hydrophobic CPTES surfaces, collagen fibers displayed a beads-on-a-string appearance. This effect has been described in other studies in which the same globular aggregates were observed for collagen type I fibrils immobilized on hydrophobic as compared to hydrophilic surfaces.[24,25,48,49]

On the other hand, on surfaces of intermediate wettability (PL-GP), collagen was adsorbed in globular aggregates. Similar behavior was observed in previous studies where the conformation of other proteins, such as fibronectin and collagen type IV, was evaluated in relation to the degree of hydrophobicity of the surfaces. In those studies, protein distribution varied from fibrillar on hydrophobic surfaces to globular aggregates on surfaces with intermediate hydrophobicity (ac ≈ 50°) due to introduction of OH^- groups on the surface.[15,23,50] Adamczak et al. reported that the foils of poly(L-lactide-*co*-glycolide), less hydrophobic than polystyrene, were covered with a granular layer of type I collagen, while collagen formed elongated structures on polystyrene.[36]

Previous studies have highlighted the effect of other parameters on collagen conformation such as the hydrodynamic flow at which the protein is deposited onto the surface,[51,52] anisotrpic chemical patterns,[53] or nanotopography.[12,25] Thus, Li et al. obtained a parallel fiber arrangement when type I collagen was adsorbed on tantalum surfaces under a constant flow, and a random collagen network in the absence of flow.[54] In the present study, collagen was deposited by immersing chemically homogeneous samples with similar roughness (RMS roughness <1 nm) in the collagen solution, and therefore, the absence of hydrodynamic flow, anisotropic

DOI: 10.1021/acsami.5b05420
ACS Appl. Mater. Interfaces 2015, 7, 20667−20677

chemical, or topographical cues is consistent with the organization of collagen into nonoriented networks.

3.4. OWLS. The OWLS studies were used to determine the amount of collagen bound on each surface, depending on the initial collagen concentration in solution. Adhered collagen was quantified on plasma-treated (PL) and silanized titanium surfaces (PL-CP, PL-GP) after 10 min (Figure 4a,b) or 16 h (Figure 4c) using either the minimum collagen concentration in solution visible in AFM studies (Figure 4) (15 μg/mL for PL, 5 μg/mL for PL-GP and 25 μg/mL for PL-CP) (Figure 4a), 25 μg/mL (Figure 4b), or 150 μg/mL collagen solution (Figure 4c).

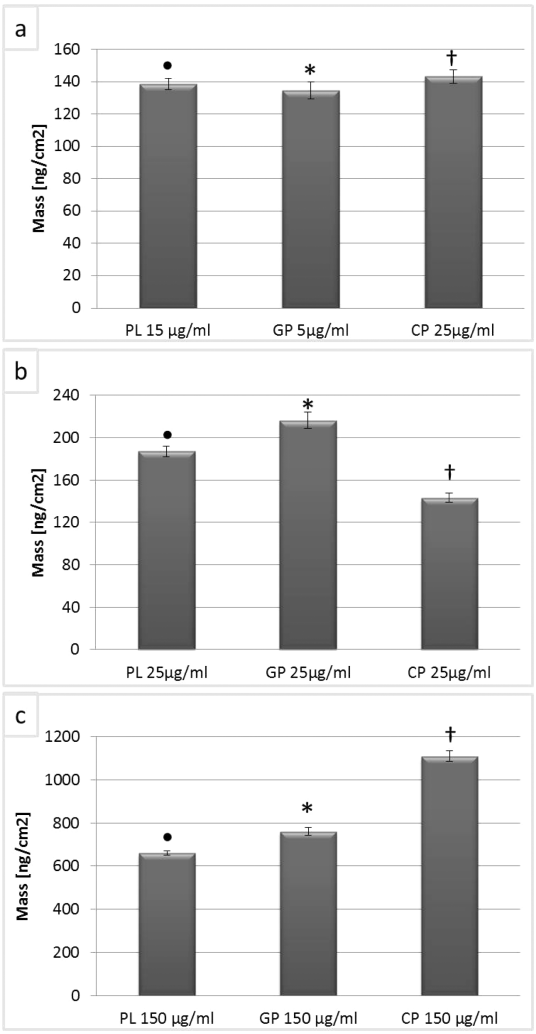

Figure 4. Quantification of the amount of type I collagen immobilized on the different modified Ti surfaces through OWLS. Amount of immobilized collagen after 10 min, with the minimum collagen concentration in solution for each surface: 15 μg/mL on PL, 5 μg/mL on PL-GP, and 25 μg/mL on PL-CP (a). Amount of immobilized collagen after 10 min, with a collagen concentration in solution of 25 μg/mL on all surfaces (b). Amount of immobilized collagen after 16 h, with a collagen concentration in solution of 150 μg/mL on all surfaces (c). The experiment was performed in triplicate for each condition (n = 3). Bars indicate standard deviation. Different symbols within each graph stand for statistically significant differences (p < 0.05).

At the minimal collagen concentrations in solution identified through AFM, PL = 15 μg/mL, PL-GP = 5 μg/mL, and PL-CP = 25 μg/mL (Figure 4a), and the surface densities of adsorbed collagen were 138.5 ± 3.4 ng/cm^2, 134.5 ± 5.2 ng/cm^2, and 143.1 ± 4.2 ng/cm^2, respectively. These results indicate that a similar amount of collagen adhered to all samples, although the initial collagen concentrations in solution were different and support the AFM ability to identify collagen adsorption at the lowest concentration of the solution. Although very similar, these amounts are statistically different (p-value <0.05), and the tendency of the adsorbed collagen follows the order PL-GP < PL < PL-CP.

After the PL-GP and PL samples were also immersed in a collagen solution with the higher concentration of 25 μg/mL for 10 min (the concentration used for PL-CP previously), the amount of adsorbed collagen increased on both surfaces, more evidently on PL-GP (216.3 ± 7.5 ng/cm^2) than on PL (186.9 ± 4.8 ng/cm^2). Therefore, when the same collagen concentration in solution was used, the amount of adsorbed protein was in the order PL-CP < PL < PL-GP, that is, with more collagen adsorbed on GPTES surfaces than on CPTES ones. These observations are in agreement with the AFM results, which suggested higher adsorption of collagen I on PL-GP compared to PL and the other silanized surface PL-CP.

By comparing the two silanes, we see that apparently the collagen reaction was more efficient with silanized GPTES samples because this required a much lower collagen concentration in solution to achieve the same amount of protein adhered on silanized CPTES samples. It is important to bear in mind that one end of the organosilane molecules must bind to the hydroxyl groups at the surface of the metal, whereas the other end binds to the collagen molecule through the specific functional group. Thus, in a first step, the hydroxyl groups present at the metal surface will act as nucleophiles toward the Si, liberating the ethoxy leaving group in solution. Once silanized, the surfaces will therefore present an available functional group suitable for further chemical modification. Then, in a second step, the nucleophiles present in type I collagen (e.g., −SH, −OH, −NH) will perform a nucleophilic attack toward the "head" functional groups of CPTES (substitution reaction) or GPTES (substitution reaction and epoxide ring opening) at specifc pHs, thus accomplishing the covalent binding. However, collagen type I molecules can be solubilized in solution only starting from acid pH and tend to precipitate when pH approaches neutrality. On the other hand, to undergo a nucleophilic attack, organosilanes require different working pH conditions depending on the nature of the functional group they bear. Specifically, CPTES and GPTES are able to undergo nucleophilic attack at various pHs that range from close to neutrality to basic conditions. Therefore, the best pH compromise for collagen solubilization and nuecleophilic attack toward both organosilanes was found to be between pH 6 and 7. For the employed working conditions, GPTES resulted to be more efficient than CPTES, probably due to the more favorable epoxide ring opening reaction over the nucleophilic substitution that takes place in the case of chlorine in CPTES.[55] Additionally, the CPTES substitution reaction produces HCl, which decreases the pH of the solution. Under acidic pH, the nucleophilic groups of collagen will be protonated, making the nucleophilic attack of silane less efficient.

Finally, when collagen was adsorbed overnight from a solution of concentration 150 μg/mL (Figure 3c), the adsorbed mass increased on silanized samples (PL-GP = 742.7 ± 17.4 ng/cm^2 and PL-CP = 1080.1 ± 25.0 ng/cm^2) as compared to the plasma-treated ones (649.8 ± 10.0 ng/cm^2), suggesting that the collagen bond with silanized surfaces was more efficient and

DOI: 10.1021/acsami.5b05420
ACS Appl. Mater. Interfaces 2015, 7, 20667−20677

stronger than with the OH groups of the samples treated only with plasma.[7,8,30,32,33] After overnight exposure, a good correlation was found between the amount of immobilized collagen and the hydrophobicity of the substrate (Figure 2), as reported in previous studies.[10,11,19,23,25,28] Additional factors that could explain the smaller amount of collagen immobilized in the PL-GP surface are the lower silanization coverage eventually limiting the amount of collagen that can be adsorbed from higher concentration solutions and that the epoxy organofunctional group of GPTES is susceptible to hydrolyzation when exposed to acidic aqueous solutions in the long term.[56] Since the reaction between silanes and collagen is performed at a pH ≈ 6, it is possible that some GPTES molecules undergo hydrolysis, consequently hampering further collagen bonding.

3.5. Fibroblast Behavior as a Function of Collagen Organization and Concentration. *3.5.1. Fibroblast Adhesion.* Figures 5–8 show the results for the percentage of attached cells, cell spreading, and circularity, as well as some morphological features, such as actin cytoskeleton, vinculin, and fibronectin expression, of the fibroblasts adhered on the modified titanium surfaces prepared under the same conditions used for the OWLS studies (Figure 4).

When the amount of adsorbed protein was similar due to adsorption from different minimal collagen concentrations in solution, PL-GP-col samples showed a higher percentage of adhered cells (69.5 ± 20.4%) (Figure 5a) with greater spreading area (412 ± 57 μm^2) (Figure 5b) than PL-col (37.6 ± 11.5% and 295 ± 62 μm^2) and PL-CP-col samples (34.1 ± 10.1% and 331 ± 58 μm^2). The analysis of circularity showed that better spreading on PL-GP-col surfaces was due to cell elongation, as indicated by lower circularity compared to the other surfaces (Figure 5c). Additionally, developed actin filaments were clearly observed only in the cytoskeleton of cells adhered onto PL-GP-col samples (Figure 6a–c).

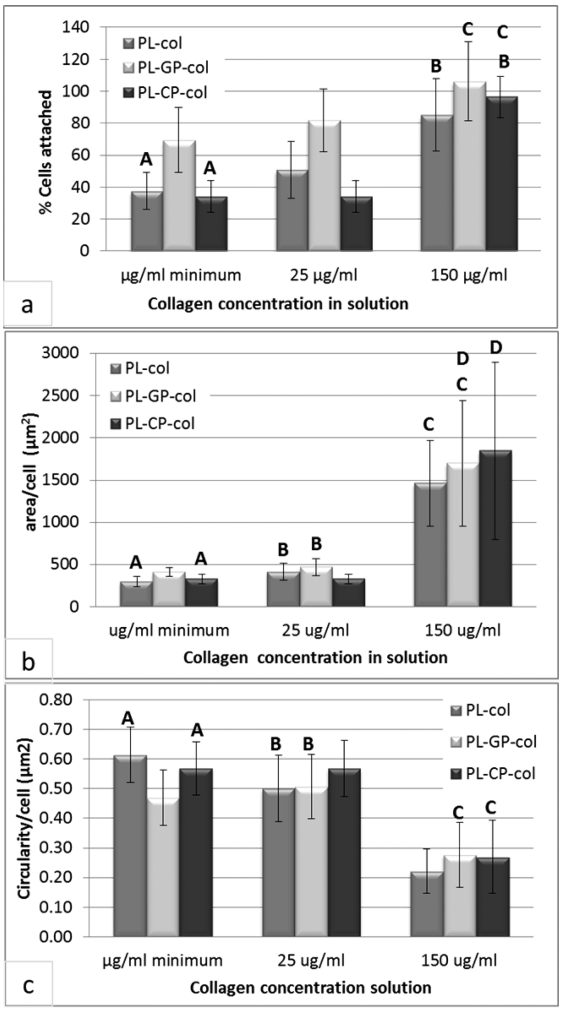

Figure 5. Percentage of attached cells (a), cell area (b), and circularity (c) of fibroblasts cultured on titanium samples biofunctionalized (PL-col, PL-GP-col, and PL-CP-col) with the minimum collagen concentrations in solution (15 μg/mL-10 min for PL, 5 μg/mL-10 min for GP, and 25 μg/mL-10 min for CP), 25 μg/mL-10 min for all surfaces, and 150 μg/mL-ON for all surfaces. Groups identified by the same letters are not statistically different ($p > 0.05$), comparison between samples within the same condition.

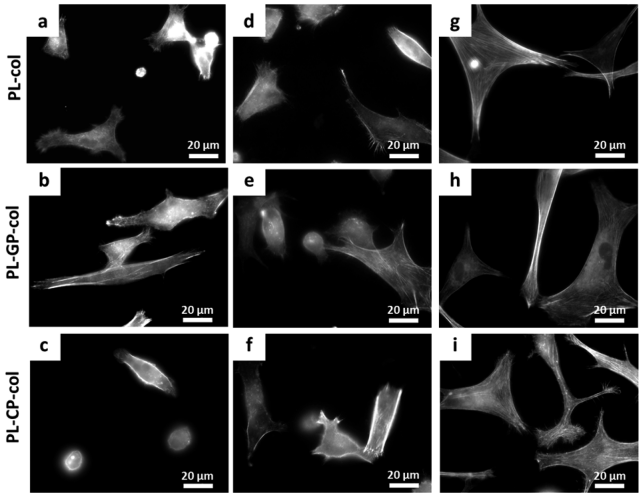

Figure 6. Actin cytoskeleton of fibroblasts cultured on biofunctionalized titanium samples PL-col, PL-GP-col, and PL-CP-col with collagen concentrations of 15 μg/mL for 10 min on PL (a), 5 μg/mL-10 min on GP (b), and 25 μg/mL-10 min on CP (c); 25 μg/mL-10 min on all surfaces (d–f) and 150 μg/mL-ON on all surfaces (g–i).

Considering that under this condition, the adsorbed amount of collagen was similar, and even lower on PL-GP-col surfaces where collagen displayed globular clusters as opposed to the fibers on the other two surfaces, one could infer that the influence of the morphology adopted by the collagen prevailed over the amount of adhered protein. In a previous study, a similar fibroblast behavior was reported on collagen-coated polystyrene and poly(L-lactide-*co*-glycolide), although the conformations adopted by collagen on these surfaces were different,[36] and the amount of collagen immobilized on each surface was not discussed. Elliot et al. reported that the spreading area of the smooth muscle cells (SMCs) was greater on collagen coated OH-terminated surfaces than CH_3-terminated surfaces. The first presented a smooth film of collagen with occasional large fibers, while the second one formed larger collagen fibers with underlying smaller collagen fibrils.[11] In our case, it seems that the globular organization of type I collagen on PL-GP-col favored the adhesion and response of fibroblast-like cells, as confirmed by the higher number of adhered cells, which were more elongated and presented a better development of their cytoskeleton; this suggests that PL-GP-col substrates favor a specific conforma-

DOI: 10.1021/acsami.5b05420
ACS Appl. Mater. Interfaces 2015, 7, 20667–20677

tion of the collagen molecule that enhances fibroblast adhesion. In fact, it is known that when proteins adsorb on a surface they adopt a given orientation that will determine the part that is in contact with the surface and the part that is exposed to the cells.[56] Additionally, after adsorption, proteins can suffer conformational changes that alter their native structure.[57,58] This, coupled with the fact that the conformation of adsorbed proteins depend on surface chemistry, can influence the domains exposed to integrins, affecting cell adhesion.[59,60]

When collagen was adsorbed from solutions with the same concentration (25 μg/mL) for 10 min on all samples, cell response remained better on PL-GP-col samples in terms of percentage of adhered cells (81.8 ± 119.6%) with respect to PL-col (50.6 ± 17.8%) and PL-CP-col (34.1 ± 10.1%) samples. This result is consistent with the previous ones, given that the final collagen concentration on PL-GP-col is increased much more with respect to the other samples. Again, well-developed actin filaments were observed only in cells adhered onto PL-GP-col samples (Figure 6d–f). No significant difference in circularity or cell area was observed between PL-GP-col (469 ± 99 μm^2) and PL-col (415 ± 101 μm^2) samples, while cells adhered on PL-CP-col samples, where the lowest amount of adhered collagen was found, showed the lowest response in terms of all cellular parameters.

Finally, when collagen was adsorbed from a 150 μg/mL solution overnight, the percentage of adhered cells increased and was higher on PL-GP-col (106.0 ± 24.7%) and PL-CP-col (96.3 ± 13.0%) samples than on PL-col (85.1 ± 22.8%). Similarly, cell spreading area was higher on collagen covalently adhered on silanized PL-CP-col (1845 ± 1046 μm^2) and PL-GP-col (1696 ± 743 μm^2) samples than on collagen physisorbed on PL-col (1461 ± 508 μm^2). The effect of the different conformations and distributions of collagen obtained on the two silanized surfaces seems to be masked by the increase of adsorbed collagen. Although the two silanized samples presented a significant difference in the amount of adsorbed collagen (1080 ng/cm^2 on PL-CP-col compared to 743 ng/cm^2 on PL-GP-col), they induced a similar cell response, thus suggesting that over a certain protein density at the surface, there is no further effect over the adhered cells, at least in the range of the studied concentrations. This further confirms that collagen organization plays a positive role on PL-GP-col samples. Concerning the actin cytoskeleton (Figure 6g–i), all surfaces promoted good cell spreading, with well-developed actin filaments in the cell cytoskeleton. It is also important to note that, under these conditions, the cell area was three-times larger than the one of cells adhered on samples with lower amounts of adsorbed collagen (Figure 5b); moreover, circularity was consistently lower (Figure 5c), indicating enhanced cell elongation on all surfaces due to the higher amount of adsorbed protein. This indicates that when the amount of adsorbed protein is high enough, cells respond better in terms of adhesion, as demonstrated in other studies.[61] The extent of cell spreading and elongation is an important parameter for the biocompatibility of substrates, being crucial for subsequent behaviors such as proliferation and cellular activation, production, and remodelling of the ECM.[6,62] Therefore, the use of a high concentration of collagen is justified to obtain a better cell response. Proliferation studies over the course of 7 days revealed similar trends for the three surfaces (Supporting Information, Figure S1).

3.5.2. Focal Points Formation and Fibronectin Fibrillogenesis. Vinculin and fibronectin expression can be observed in Figures 7 and 8 for all the evaluated conditions: minimal collagen concentrations, 25 μg/mL for 10 min, and 150 μg/mL

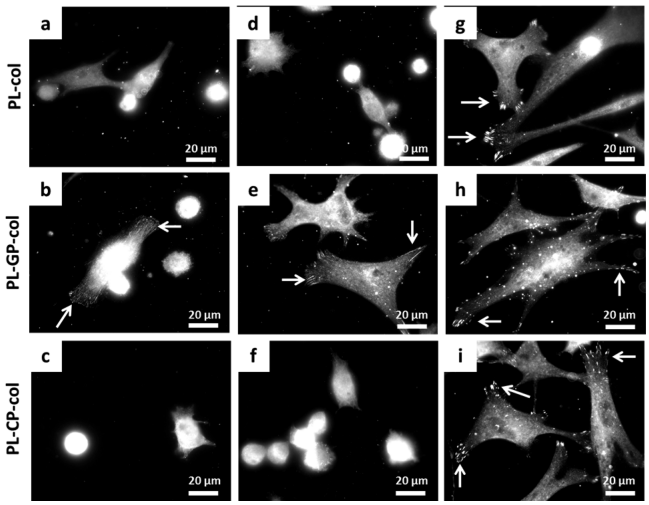

Figure 7. Vinculin expression of fibroblasts cultured on titanium samples biofunctionalized (PL-col, PL-GP-col, and PL-CP-col) with collagen concentrations of 15 μg/mL-10 min for PL (a), 5 μg/mL-10 min for GP (b), and 25 μg/mL-10 min for CP (c); 25 μg/mL-10 min for all surfaces (d–f) and 150 μg/mL-ON for all surfaces (g–i). Focal points and stress fibers indicated by arrows.

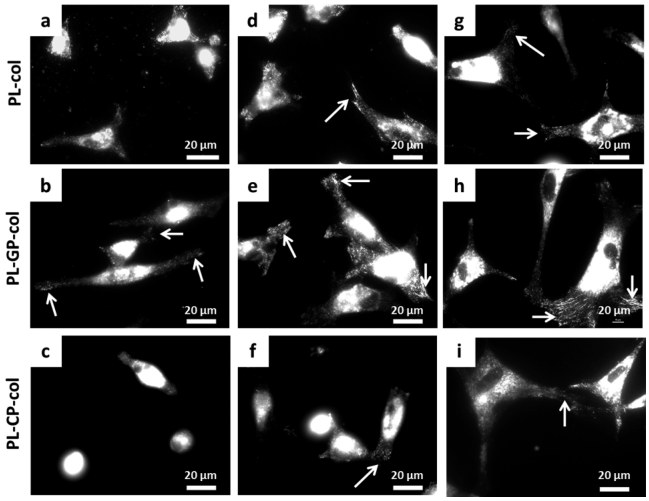

Figure 8. Fibronectin expression of fibroblasts cultured on titanium samples biofunctionalized (PL-col, PL-GP-col, and PL-CP-col) with collagen concentrations of 15 μg/mL-10 min for PL (a), 5 μg/mL-10 min for GP (b), and 25 μg/mL-10 min for CP (c); 25 μg/mL-10 min for all surfaces (d–f) and 150 μg/mL-ON for all surfaces (g–i). Early fibril formation indicated by arrows. Higher magnifications of the fibronectin fibrils are shown in Supporting Information, Figure S2.

overnight for all surfaces. When the amount of adsorbed collagen was similar, at the minimal solution concentrations (Figure 7a–c), some cells with developed focal points could be observed only on PL-GP-col surfaces, confirming that this surface enhances the early adhesion of fibroblasts. Similarly, fibroblasts secreted fibronectin and started to organize it into fibers only on PL-GP-col surfaces (Figure 8a–c and Supporting Information, Figures S2 and S3). The presence of fibronectin fibers at the cell filopodia has been attributed to early secretion and organization of fibronectin by cells[15,23,63] and is related to

DOI: 10.1021/acsami.5b05420
ACS Appl. Mater. Interfaces 2015, 7, 20667–20677

cell capacity to secrete and organize an early matrix, which eventually affects the biocompatibility of a surface.[64] On the other hand, on PL-col and PL-CP-col surfaces, fibronectin expression was observed only inside the cell, and no fibers were formed. When collagen concentration in solution was increased to 25ug/mL for 10 min for all samples (Figure 7d–f), the formation of focal points and organization of small fibronectin fibrils were again observed only for fibroblasts adhered on PL-GP-col samples (Figure 7e). The assembly of fibronectin matrix is the initial step that orchestrates the assembly of other ECM proteins and promotes cell adhesion, migration, and signaling.[65] Our study demonstrates that type I collagen regulates the beginning of the short fibronectin fibers formation, which is the initial step of the extracellular fibronectin matrix assembly. Surfaces that provide for a better cell adhesion, such as PL-GP-col, allow also for a faster organization of secreted fibronectin. Moreover, fibronectin has domains for interaction with other ECM proteins including collagen.[65−67] Studies performed by Dzamba et al. also reported that the α1(I) chain of collagen contains a binding fibronectin region between amino acids residues 757 and 791, which has an influence on the assembly of fibronectin into fibrils.[68]

The results obtained so far suggest that at low collagen concentrations, protein conformation on PL-GP-col samples favors cell adhesion and matrix formation; we hypothesize that the cluster organization of collagen provides the adequate signals, which stimulate matrix formation activity of fibroblast cultured on PL-GP-col samples. Particularly, the globular organization of collagen upon immobilization on this surface likely presents binding sites for the main collagen integrins of dermal fibroblasts ($\alpha_1\beta_1$, $\alpha_2\beta_1$)[69] in a conformation that allows integrin clustering and focal adhesion formation even at low protein concentrations. Interestingly, the distance between the globular clusters on PL-GP-col samples is in range of 70 nm, which has been indicated as the critical local interligand spacing for integrin clustering and cell adhesion.[70] Hence, GPTES silanization seems to be the treatment that provides an adequate collagen conformation for enhanced fibroblast response.

However, for longer immersion times and higher collagen concentration, a similarly good cell response, in terms of focal adhesion points (Figure 7g–i) and fibronectin fibrillogenesis (Figure 8g–i and Supporting Information, Figures S2 and S3), was observed on all samples. The increase of adsorbed collagen seems in this case to mask the effect of the different collagen morphologies.

4. CONCLUSIONS

The collagen morphology on each of the studied surfaces was dependent on the degree of surface hydrophobicity. PL (hydrophilic) and PL-CP samples (hydrophobic) showed collagen organization in fibrillar networks. In the case of PL-CP, fibers were in turn formed by little globules, adopting a beads-on-a-string appearance, and increased in thickness with increasing collagen concentration, which was attributed to the high hydrophobicity of this type of surface. On the other hand, PL-GP samples, with an intermediate hydrophobic character, induced collagen organization into clusters, which increased in size with increasing protein concentration in solution.

The amount of collagen adhered on modified titanium surfaces was dependent on surface chemistry and the duration of the immersion into the protein solution. For lower collagen concentrations in solution (<25 μg/mL) and 10 min of immersion, the amount of collagen was higher on PL-GP surfaces than on PL-CP and PL surfaces. The differences between these surfaces were the functional groups that interact with the collagen. GPTES silane has an epoxy as a functional group, while CPTES silane has a chlorine, and samples treated with plasma have hydroxyl groups on their surfaces, which appears to influence the kinetics of the adsorption. Conversely, for high collagen concentration (~150 μg/mL) and long immersion time, the amount of adhered collagen is higher on PL-CP than on PL-GP samples, probably due to the nature of the reaction kinetics and because the epoxy group of GPTES silane is prone to hydrolyzation in acid medium in the long term.

The samples where collagen was organized in globular clusters (PL-GP samples) supported a faster and better fibroblast adhesion as well as better cell spreading, focal adhesions formation, and more pronounced fibronectin fibrillogenesis. Collagen is likely to be immobilized on these surfaces in a conformation that enhances cell response. When higher amounts of collagen were adsorbed, the effect of the morphology of collagen on fibroblast response was partially masked.

■ ASSOCIATED CONTENT

Supporting Information

The Supporting Information is available free of charge on the ACS Publications website at DOI: 10.1021/acsami.5b05420.

Proliferation of human dermal fibroblasts; high-magnification images of fibronectin fibrils; quantification of average number per cell and length of early fibronectin fibrils formed on different surfaces (PDF)

■ AUTHOR INFORMATION

Corresponding Author

*E-mail: maria.pau.ginebra@upc.edu. Phone: +34934017706. Mobile Phone +34638033329.

Author Contributions

[§]These authors contributed equally.

Notes

The authors declare no competing financial interest.

■ ACKNOWLEDGMENTS

The authors acknowledge the Spanish Government for financial support through Project No. MAT2012-38438-C03, cofunded by the EU through European Regional Development Funds. Support for the research of M.-P.G. was received through the "ICREA Academia" award for excellence in research, funded by the Generalitat de Catalunya. N.M.P. acknowledges a mobility grant from CIBER-BBN. M.S.S. acknowledges support from ERC through HealInSynergy (306990).

■ REFERENCES

(1) Guillem-Marti, J.; Delgado, L.; Godoy-Gallardo, M.; Pegueroles, M.; Herrero, M.; Gil, F. J. Fibroblast Adhesion and Activation onto Micro-Machined Titanium Surfaces. *Clin. Oral Impl. Res.* **2013**, *24*, 770−780.

(2) Myshin, H. L.; Wiens, J. P. Factors Affecting Soft Tissue around Dental Implants: A Review of the Literature. *J. Prosthet. Dent.* **2005**, *94*, 440−444.

(3) Werner, S.; Huck, O.; Frisch, B.; Vautier, D.; Elkaim, R.; Voegel, J.-C.; Brunel, G.; Tenenbaum, H. The Effect of Microstructured Surfaces and Laminin-Derived Peptide Coatings on Soft Tissue

DOI: 10.1021/acsami.5b05420
ACS Appl. Mater. Interfaces 2015, 7, 20667−20677

Interactions with Titanium Dental Implants. *Biomaterials* **2009**, *30*, 2291−2301.
(4) Wilson, C. J.; Clegg, R. E.; Leavesley, D. I.; Pearcy, M. J. Mediation of Biomaterial-Cell Interactions by Adsorbed Proteins: a Review. *Tissue Eng.* **2005**, *11*, 1−18.
(5) Campillo-Fernández, A. J.; Unger, R. E.; Peters, K.; Halstenberg, S.; Santos, M.; Salmerón Sánchez, M.; Meseguer Dueñas, J. M.; Monleón Pradas, M.; Gómez Ribelles, J. L.; Kirkpatrick, C. J. Analysis of the Biological Response of Endothelial and Fibroblast Cells Cultured on Synthetic Scaffolds with Various Hydrophilic/Hydrophobic Ratios: Influence of Fibronectin Adsorption and Conformation. *Tissue Eng., Part A* **2009**, *15*, 1331−1341.
(6) Bacakova, L.; Filova, E.; Parizek, M.; Ruml, T.; Svorcik, V. Modulation of Cell Adhesion, Proliferation and Differentiation on Materials Designed for Body Implants. *Biotechnol. Adv.* **2011**, *29*, 739−767.
(7) Schliephake, H.; Scharnweber, D. Chemical and Biological Functionalization of Titanium for Dental Implants. *J. Mater. Chem.* **2008**, *18*, 2404−2414.
(8) Müller, R.; Abke, J.; Schnell, E.; Scharnweber, D.; Kujat, R.; Englert, C.; Taheri, D.; Nerlich, M.; Angele, P. Influence of Surface Pretreatment of Titanium- and Cobalt-Based Biomaterials on Covalent Immobilization of Fibrillar Collagen. *Biomaterials* **2006**, *27*, 4059−4068.
(9) Sun, T.; Norton, D.; Ryan, A. J.; MacNeil, S.; Haycock, J. W. Investigation of Fibroblast and Keratinocyte Cell-Scaffold Interactions Using a Novel 3D Cell Culture System. *J. Mater. Sci.: Mater. Med.* **2007**, *18*, 321−328.
(10) Ying, P.; Jin, G.; Tao, Z. Competitive Adsorption of Collagen and Bovine Serum Albumin—Effect of the Surface Wettability. *Colloids Surf., B* **2004**, *33*, 259−263.
(11) Elliott, J. T.; Woodward, J. T.; Umarji, A.; Mei, Y.; Tona, A. The Effect of Surface Chemistry on the Formation of Thin Films of Native Fibrillar Collagen. *Biomaterials* **2007**, *28*, 576−585.
(12) Dufrêne, Y. F.; Marchal, T. G.; Rouxhet, P. G Influence of Substratum Surface Properties on the Organization of Adsorbed Collagen Films: In Situ Characterization by Atomic Force Microscopy. *Langmuir* **1999**, *15*, 2871−2878.
(13) Roach, P.; Farrar, D.; Perry, C. C. Interpretation of Protein Adsorption: Surface-Induced Conformational Changes. *J. Am. Chem. Soc.* **2005**, *127*, 8168−8173.
(14) Sethuraman, A.; Han, M.; Kane, R. S.; Belfort, G. Effect of Surface Wettability on the Adhesion of Proteins. *Langmuir* **2004**, *20*, 7779−7788.
(15) Gugutkov, D.; Altankov, G.; Rodríguez Hernández, J. C.; Monleón Pradas, M.; Salmerón Sánchez, M. Fibronectin Activity on Substrates with Controlled -OH Density. *J. Biomed. Mater. Res., Part A* **2010**, *92A*, 322−331.
(16) Bergkvist, M.; Carlsson, J.; Oscarsson, S. Surface-Dependent Conformations of Human Plasma Fibronectin Adsorbed to Silica, Mica, and Hydrophobic Surfaces, Studied with Use of Atomic Force Microscopy. *J. Biomed. Mater. Res.* **2003**, *64A*, 349−356.
(17) Rodríguez Hernández, J. C.; Rico, P.; Moratal, D.; Monleón Pradas, M.; Salmerón-Sánchez, M. Fibrinogen Patterns and Activity on Substrates with Tailored Hydroxy Density. *Macromol. Biosci.* **2009**, *9*, 766−775.
(18) Rodríguez Hernández, J. C.; Salmerón Sánchez, M.; Soria, J. M.; Gómez Ribelles, J. L.; Monleón Pradas, M. Substrate Chemistry-Dependent Conformations of Single Laminin Molecules on Polymer Surfaces are Revealed by the Phase Signal of Atomic Force Microscopy. *Biophys. J.* **2007**, *93*, 202−207.
(19) Keselowsky, B. G.; Collard, D. M.; García, A. J. Surface Chemistry Modulates Fibronectin Conformation and Directs Integrin Binding and Specificity to Control Cell Adhesion. *J. Biomed. Mater. Res.* **2003**, *66A*, 247−259.
(20) Arima, Y.; Iwata, H. Effect of Wettability and Surface Functional Groups on Protein Adsorption and Cell Adhesion Using Well-Defined Mixed Self-Assembled Monolayers. *Biomaterials* **2007**, *28*, 3074−3082.
(21) Tang, L.; Thevenot, P.; Hu, W. Surface Chemistry Influence Implant Biocompatibility. *Curr. Top. Med. Chem.* **2008**, *8*, 270−280.
(22) Arima, Y.; Iwata, H. Effects of Surface Functional Groups on Protein Adsorption and Subsequent Cell Adhesion Using Self-Assembled Monolayers. *J. Mater. Chem.* **2007**, *17*, 4079−4089.
(23) Llopis-Hernández, V.; Rico, P.; Ballester-Beltrán, J.; Moratal, D.; Salmerón-Sánchez, M. Role of Surface Chemistry in Protein Remodeling at the Cell-Material Interface. *PLoS One* **2011**, *6* (5), e19610.
(24) Dupont-Gillain, C. C.; Pamula, E.; Denis, F. a; De Cupere, V. M.; Dufrêne, Y. F.; Rouxhet, P. G. Controlling the Supramolecular Organisation of Adsorbed Collagen Layers. *J. Mater. Sci.: Mater. Med.* **2004**, *15*, 347−353.
(25) Denis, F. A.; Hanarp, P.; Sutherland, D. S.; Gold, J.; Mustin, C.; Rouxhet, P. G.; Dufrene, Y. F. Protein Adsorption on Model Surfaces with Controlled Nanotopography and Chemistry. *Langmuir* **2002**, *18*, 819−828.
(26) Miranda-Coelho, N.; González-García, C.; Planell, J.; Salmerón-Sánchez, M.; Altankov, G. Different Assembly of Type IV Collagen on Hydrophilic and Hydrophobic Substrata Alters Endothelial Cells Interaction. *Eur. Cell Mater.* **2010**, *19*, 262−272.
(27) Keresztes, Z.; Rouxhet, P. G.; Remacle, C.; Dupont-Gillain, C. Supramolecular Assemblies of Adsorbed Collagen Affect the Adhesion of Endothelial Cells. *J. Biomed. Mater. Res., Part A* **2006**, *76A*, 223−233.
(28) Chen, C.; Zhang, S.-M.; Lee, I.-S. Immobilizing Bioactive Molecules onto Titanium Implants to Improve Osseointegration. *Surf. Coat. Technol.* **2013**, *228* (Suppl. 1), S312−S317.
(29) Marín-Pareja, N.; Salvagni, E.; Guillem-Marti, J.; Aparicio, C.; Ginebra, M.-P. Collagen-Functionalised Titanium Surfaces for Biological Sealing of Dental Implants: Effect of Immobilisation Process on Fibroblasts Response. *Colloids Surf., B* **2014**, *122*, 601−610.
(30) Bagno, A.; Piovan, A.; Dettin, M.; Chiarion, A.; Brun, P.; Gambaretto, R.; Fontana, G.; Di Bello, C.; Palù, G.; Castagliuolo, I. Human Osteoblast-Like Cell Adhesion on Titanium Substrates Covalently Functionalized with Synthetic Peptides. *Bone* **2007**, *40*, 693−699.
(31) Middleton, C. A.; Pendegrass, C. J.; Gordon, D.; Jacob, J.; Blunn, G. W. Fibronectin Silanized Titanium Alloy: A Bioinductive and Durable Coating to Enhance Fibroblast Attachment in Vitro. *J. Biomed. Mater. Res., Part A* **2007**, *83A*, 1032−1038.
(32) Sargeant, T. D.; Rao, M. S.; Koh, C.-Y.; Stupp, S. I. Covalent Functionalization of NiTi Surfaces with Bioactive Peptide Amphiphile Nanofibers. *Biomaterials* **2008**, *29*, 1085−1098.
(33) Schreiber, F. Structure and Growth of Self-Assembling Monolayers. *Prog. Surf. Sci.* **2000**, *65*, 151−257.
(34) Morra, M.; Cassinelli, C.; Cascardo, G.; Cahalan, P.; Cahalan, L.; Fini, M.; Giardino, R. Surface Engineering of Titanium by Collagen Immobilization. Surface Characterization and in Vitro and in Vivo Studies. *Biomaterials* **2003**, *24*, 4639−4654.
(35) Hauser, J.; Zietlow, J.; Köller, M.; Esenwein, S. a; Halfmann, H.; Awakowicz, P.; Steinau, H. U. Enhanced Cell Adhesion to Silicone Implant Material through Plasma Surface Modification. *J. Mater. Sci.: Mater. Med.* **2009**, *20*, 2541−2548.
(36) Adamczak, M.; Scisłowska-Czarnecka, A.; Genet, M. J.; Dupont-Gillain, C. C.; Pamuła, E. Surface Characterization, Collagen Adsorption and Cell Behaviour on Poly(L-Lactide-Co-Glycolide). *Acta Bioeng. Biomech.* **2011**, *13*, 63−75.
(37) Jorge-Herrero, E.; Fernández, P.; Turnay, J.; Olmo, N.; Calero, P.; García, R.; Freile, I.; Castillo-Olivares, J. Influence of Different Chemical Cross-Linking Treatments on The Properties of Bovine Pericardium and Collagen. *Biomaterials* **1999**, *20*, 539−545.
(38) Pegueroles, M.; Gil, F.; Planell, J.; Aparicio, C. The Influence of Blasting and Sterilization on Static and Time-Related Wettability and Surface-Energy Properties of Titanium Surfaces. *Surf. Coat. Technol.* **2008**, *202*, 3470−3479.
(39) Diéguez, L.; Darwish, N.; Mir, M.; Martínez, E.; Moreno, M.; Samitier, J. Effect of the Refractive Index of Buffer Solutions in Evanescent Optical Biosensors. *Sens. Lett.* **2009**, *7*, 851−855.

DOI: 10.1021/acsami.5b05420
ACS Appl. Mater. Interfaces 2015, 7, 20667−20677

(40) Berginski, M. E.; Gomez, S. M. The Focal Adhesion Analysis Server: a Web Tool for Analyzing Focal Adhesion Dynamics. *F1000Research* **2013**, *2*, 68.
(41) Vanterpool, F. A.; Cantini, M.; Seib, F. P.; Salmerón-Sánchez, M. A Material-Based Platform to Modulate Fibronectin Activity and Focal Adhesion Assembly. *BioRes. Open Access* **2014**, *3*, 286−296.
(42) Martin, H.; Schulz, K.; Bumgardner, J.; Walters, K. An XPS Study on the Attachment of Triethoxsilylbutyraldehyde to Two Titanium Surfaces as a Way to Bond Chitosan. *Appl. Surf. Sci.* **2008**, *254*, 4599−4605.
(43) Xiao, S. J.; Textor, M.; Spencer, N. D.; Sigrist, H. Covalent Attachment of Cell-Adhesive, (Arg-Gly-Asp)-Containing Peptides to Titanium Surfaces. *Langmuir* **1998**, *14*, 5507−5516.
(44) Salvagni, E.; Berguig, G.; Engel, E.; Rodriguez-Cabello, J. C.; Coullerez, G.; Textor, M.; Planell, J. a; Gil, F. J.; Aparicio, C. A Bioactive Elastin-Like Recombinamer Reduces Unspecific Protein Adsorption and Enhances Cell Response on Titanium Surfaces. *Colloids Surf., B* **2014**, *114*, 225−233.
(45) Serro, A.; Saramago, B. Influence of Sterilization on the Mineralization of Titanium Implants Induced by Incubation in Various Biological Model Fluids. *Biomaterials* **2003**, *24*, 4749−4760.
(46) Arkles, B. Hydrophobicity, Hydrophilicity and Silanes. *Paint Coatings Ind. Mag.* **2006**, *22*, 114.
(47) Shoulders, M. D.; Raines, R. T. Collagen Structure and Stability. *Annu. Rev. Biochem.* **2009**, *78*, 929−958.
(48) De Cupere, V. M.; Rouxhet, P. G. Collagen Films Adsorbed on Native and Oxidized Poly (Ethylene Terephtalate): Morphology after Drying. *Surf. Sci.* **2001**, *491*, 395−404.
(49) Pamula, E.; De Cupere, V.; Dufrêne, Y. F.; Rouxhet, P. G. Nanoscale Organization of Adsorbed Collagen: Influence of Substrate Hydrophobicity and Adsorption Time. *J. Colloid Interface Sci.* **2004**, *271*, 80−91.
(50) Coelho, N. M.; González-Garcia, C.; Salmerón-Sánchez, M.; Altankov, G. Arrangement of Type IV Collagen and Laminin on Substrates with Controlled Density of − OH Groups. *Tissue Eng., Part A* **2011**, *17*, 2245−2257.
(51) Dong, M.; Hovgaard, M. B.; Mamdouh, W.; Xu, S.; Otzen, D. E.; Besenbacher, F. AFM-Based Force Spectroscopy Measurements of Mature Amyloid Fibrils of the Peptide Glucagon. *Nanotechnology* **2008**, *19*, 384013.
(52) Dong, M.; Sahin, O. A Nanomechanical Interface to Rapid Single-Molecule Interactions. *Nat. Commun.* **2011**, *2*, 247.
(53) Denis, F. A.; Pallandre, A.; Nysten, B.; Jonas, A. M.; Dupont-Gillain, C. C. Alignment and Assembly of Adsorbed Collagen Molecules Induced by Anisotropic Chemical Nanopatterns. *Small* **2005**, *1*, 984−991.
(54) Li, Y.; Zhang, S.; Guo, L.; Dong, M.; Liu, B.; Mamdouh, W. Collagen Coated Tantalum Substrate for Cell Proliferation. *Colloids Surf., B* **2012**, *95*, 10−15.
(55) Ege, S. N. *Organic Chemistry. Structure and Reactivity*, 4th ed.; Stratton, R., Warne, S., Eds.; Houghton Mifflin Company: New York, 1999.
(56) Xu, H.; Zhao, X.; et al. Orientation of A Monoclonal Antibody Absorbed at the Solid/Solution Interface: A Combined Study Using Atomic Force Micrsocopy and Neutron Refelctivity. *Langmuir* **2006**, *22*, 6313−6320.
(57) Gray, J. J. The Interaction of Proteins with Solid Surfaces. *Curr. Opin. Struct. Biol.* **2004**, *14*, 110−115.
(58) Rabe, M.; Verdes, D.; Seeger, S. Understanding Protein Adsorption Phenomena at Solid Surfaces. *Adv. Colloid Interface Sci.* **2011**, *162*, 87−106.
(59) Keselowsky, B. G.; Collard, D. M.; García, A. J. Surface Chemistry Modulates Focal Adhesion Composition and Signaling through Changes in Integrin Binding. *Biomaterials* **2004**, *25*, 5947−5954.
(60) Rico, P.; Cantini, M.; Altankov, G.; Salmerón-Sánchez, M. Matrix Protein Interactions with Synthetic Surfaces. In *Polymers in Regenerative Medicine: Biomedical Applications from Nano- to Macro-Structures*; Pradas, M. M., Vicent, M. J., Eds.; John Wiley & Sons: Hoboken, NJ, 2014.
(61) Schuler, M.; Owen, G. R.; Hamilton, D. W.; de Wild, M.; Textor, M.; Brunette, D. M.; Tosatti, S. G. P. Biomimetic Modification of Titanium Dental Implant Model Surfaces Using the RGDSP-Peptide Sequence: A Cell Morphology Study. *Biomaterials* **2006**, *27*, 4003−4015.
(62) Zhao, Y.; Yao, Y.; Liu, W.; Zheng, C.; Li, S. Fibroblast Adhesion and Proliferation on a New β Type Ti-39Nb-13Ta-4. 6Zr Alloy for Biomedical Application. *J. Mater. Sci. Technol.* **2006**, *22*, 205−210.
(63) Coelho, N. M.; Salmerón-Sánchez, M.; Altankov, G. Fibroblasts Remodeling of Type IV Collagen at Biomaterials Interface. *Biomater. Sci.* **2013**, *1*, 494−502.
(64) Salmerón-Sánchez, M.; Altankov, G. Cell-Protein-Material Interaction in Tissue Engineering. In *Tissue Engineering*; Eberli, D., Ed.; In-Teh: Vukovar, Croatia, 2010; pp 77−102.
(65) Singh, P.; Carraher, C.; Schwarzbauer, J. E. Assembly of Fibronectin Extracellular Matrix. *Annu. Rev. Cell Dev. Biol.* **2010**, *26*, 397−419.
(66) Mao, Y.; Schwarzbauer, J. E. Fibronectin Fibrillogenesis, a Cell-Mediated Matrix Assembly Process. *Matrix Biol.* **2005**, *24*, 389−399.
(67) Schwarzbauer, J. E.; DeSimone, D. W. Fibronectins, their Fibrillogenesis, and In Vivo Functions. *Cold Spring Harbor Perspect. Biol.* **2011**, *3*, 1−19.
(68) Dzamba, B. J.; Wu, H.; Jaenisch, R.; Peters, D. M. Fibronectin Binding Site in Type I Collagen Regulates Fibronectin Fibril Formation. *J. Cell Biol.* **1993**, *121*, 1165−1172.
(69) Gullberg, D.; Gehisen, K. R.; Turner, D. C.; Ahlén, K.; Zijenah, L. S.; Barnes, M. J.; Rubin, K. Analysis of Alpha 1 Beta 1, Alpha 2 Beta 1 and Alpha 3 Beta 1 Integrins in Cell−Collagen Interactions: Identification of Conformation Dependent Alpha 1 Beta 1 Binding Sites in Collagen Type I. *EMBO J.* **1992**, *11*, 3865−3873.
(70) Huang, J.; Grater, S. V.; Corbellini, F.; Rinck, S.; Bock, E.; Kemkemer, R.; Kessler, H.; Ding, J.; Spatz, J. P. Impact of order and disorder in RGD nanopatterns on cell adhesion. *Nano Lett.* **2009**, *9*, 1111−1116.

DOI: 10.1021/acsami.5b05420
ACS Appl. Mater. Interfaces 2015, 7, 20667−20677